

Hyperfine magnetic field in ferromagnetic graphite

Jair C. C. Freitas,¹ Wanderlã L. Scopel,^{1,2} Wendel S. Paz,¹ Leandro V. Bernardes,³ Francisco E. Cunha-Filho,³ Carlos Speglich,³ Fernando M. Arajo-Moreira,³ Damjan Pelc,⁴ Toni Cvitani,⁴ and Miroslav Poek⁴

¹⁾ *Departamento de Física, Universidade Federal do Espírito Santo, Vitória, Brazil^{a)}*

²⁾ *Departamento de Ciências Exatas, Universidade Federal Fluminense, Volta Redonda, RJ, Brazil^{b)}*

³⁾ *Department of Physics, Federal University of São Carlos, P.O. Box 676, 13565-905, São Carlos, SP, Brazil*

⁴⁾ *Department of Physics, Faculty of Science, University of Zagreb, Bijenika 32, HR-10000, Zagreb, Croatia*

(Dated: 20 June 2021)

Information on atomic-scale features is required for a better understanding of the mechanisms leading to magnetism in non-metallic, carbon-based materials. This work reports a direct evaluation of the hyperfine magnetic field produced at ^{13}C nuclei in ferromagnetic graphite by nuclear magnetic resonance (NMR). The experimental investigation was made possible by the results of first-principles calculations carried out in model systems, including graphene sheets with atomic vacancies and graphite nanoribbons with edge sites partially passivated by oxygen. A similar range of maximum hyperfine magnetic field values (18-21T) was found for all systems, setting the frequency span to be investigated in the NMR experiments; accordingly, a significant ^{13}C NMR signal was detected close to this range without any external applied magnetic field in ferromagnetic graphite.

The occurrence of magnetism in carbon materials has been the subject of many investigations and some controversy along the past two decades. An enormous interest in the possibility of producing magnetic materials predominantly consisting of carbon (perhaps with other light elements such as hydrogen and oxygen, but free from metallic elements) exists mainly due to the potential for applications of biocompatible magnetic materials to be used in drug delivery and magnetic resonance imaging, among others. Moreover, the design of graphene-based spintronics devices would greatly benefit from the definitive establishment and a deep understanding of the mechanisms leading to magnetism in carbon materials^{1,2}. Recent experimental evidences of magnetic properties (with reports of ferromagnetic order in some cases) of carbon-based materials include irradiated graphite, nanocarbons, oxygen-containing carbons and point defects in graphene^{1,3-7}. From the theoretical point of view, magnetism in graphene and related materials has been universally associated with the occurrence of defects such as atomic vacancies, chemisorbed species (such as fluorine, hydrogen and oxygen) and edge sites^{1,3,5,6,8}. In spite of this, there is still some skepticism about the possibility of intrinsic magnetic effects in carbon-based materials, due to the ubiquitously questioned presence in experimentally-produced samples of minor amounts of iron or other metallic impurities that could be the actual source of magnetism^{1,3}.

If intrinsic magnetism is indeed a feature of carbon-based materials, then it would be possible in principle to look for the effects due to atomic magnetic moments

on the respective atomic nuclei, i.e., a hyperfine interaction (HFI) should hopefully be detectable. In the case of systems possessing magnetic order, a strong hyperfine magnetic field (B_{hf}) at the atomic nuclei could be anticipated. Therefore, evidences of the HFI and measurements of B_{hf} are highly desirable for a better understanding of the issue of magnetism in carbon-based materials, allowing the assessment of information on the source of magnetism from a local perspective. Besides its importance from a fundamental point of view, the study of the HFI is of high relevance for possible applications of graphene and related materials in spintronics and quantum information processing, since the HFI is considered the most important mechanism of electron spin decoherence in these systems⁹. Moreover, the HFI plays a central role in many recent proposals of solid-state quantum computers^{10,11}. There were some theoretical calculations regarding the HFI in graphene and related materials^{9,12} and also a number of experiments were tried to detect B_{hf} by using techniques such as muon spin spectroscopy (SR)¹³ and perturbed angular distribution (PAD)¹⁴. In none of these reports, however, any clue about the B_{hf} value at ^{13}C nuclei (Among the naturally occurring carbon nuclides, ^{13}C is the only one with non-zero nuclear spin ($I = 1/2$) and therefore ^{13}C nuclei are sensitive to the magnetic HFI in magnetic carbon-based materials) in a truly ferromagnetic carbon material was ever reported.

Paralleling the former reports about the HFI in magnetic metals such as iron, cobalt and nickel^{15,17}, the direct measurement of B_{hf} at ^{13}C nuclei should be possible in a ferromagnetic carbon-based material by means of zero-field nuclear magnetic resonance (NMR). However, contrary to the case of NMR experiments performed in diamagnetic or paramagnetic materials under strong applied magnetic fields, the main difficulty in zero-field NMR experiments is the lack of information about the

^{a)} Electronic mail: jairccfreitas@yahoo.com.br

^{b)} Electronic mail: wlscopel@gmail.com

possible frequency range where the resonance is to be found. We thus decided to carry out a methodical investigation about the HFI in a ferromagnetic carbon-based material, searching for the resonance frequency and aiming to determine the value of B_{hf} at ^{13}C nuclei by means of zero-field NMR. The material chosen to perform the experiments was ferromagnetic graphite, produced by controlled oxidation of high-purity graphite¹⁸. As previously described^{7,19,20}, this material can be produced in bulk quantities ($\sim 50\text{mg}$) and presents ferromagnetic order at room temperature and below. The maximum amounts of metallic impurities detected in this material are well below the limits required to account for its overall magnetization, pointing to a genuinely carbon-originated magnetism¹⁹. The magnetic properties of this material are related to the defects introduced in the graphite lattice by the oxygen attack, in agreement with recent theoretical calculations performed in graphite nanoribbons with edges partially passivated by oxygen atoms⁵. The sample selected for the NMR experiments showed a well-defined hysteresis loop in a magnetization versus applied magnetic field measurement conducted at low temperature (1.8K), with coercive field of ca. 500Oe, clearly indicating its ferromagnetic character.

After choosing a suitable ferromagnetic carbon-based material, the next quest was to search for the zero-field NMR signal. The NMR experiments were conducted at low temperature (1.5K), so as to maximize the sample magnetization and to minimize transverse relaxation effects in a two-pulse spin echo pulse sequence^{18,21}. Without any clue about where to look for the resonance, it would be practically impossible to successfully pursue this task. Thus, a series of first-principles calculations based on the density functional theory (DFT) were carried out in model systems built to somewhat reproduce the local features of the structure of ferromagnetic graphite. The model systems chosen for the DFT calculations included graphene sheets with isolated or multiple single atomic vacancies as well as graphite nanoribbons with oxygen atoms adsorbed at the zigzag edge sites¹⁸. These systems are known from previous reports^{1,4-6,8,22} to give rise to magnetic moments localized at carbon atoms, with indications of a ferromagnetic ground state in some cases^{5,22}, and thus they were considered good candidates for the initial calculations of B_{hf} at ^{13}C nuclei.

A summary of the results of the DFT calculations is presented in Table I. The first noticeable aspect of these results was that all B_{hf} values fell into the same range, 18-21T, despite the different types of defects giving rise to magnetism in vacancy-containing graphene sheets and in oxygen-containing graphite nanoribbons. This is an indication that the B_{hf} values here reported are indeed characteristic of carbon sites with localized magnetic moments in carbon-based systems. As it should be expected, the largest B_{hf} values in each system were found at the sites also presenting the highest net spin densities and, thus, the largest atomic magnetic moments, as illustrated

in Fig. 1 for some of the studied systems.

TABLE I. Calculated hyperfine magnetic field (B_{hf}) in ferromagnetic carbon-based systems. The reported values correspond to the average taken over the sites where the largest magnetic moments were located in each system.

System	B_{hf} (T)
Graphene sheet with one single vacancy (System A ^a)	19.4
Graphene sheet with one single vacancy (System B ^b)	18.8
Graphene sheet with two single vacancies (System C ^c)	18.3
Graphene sheet with two single vacancies (System D ^d)	20.2
Graphite nanoribbon (System E ^e)	20.8

^a System A: Supercell with 71 carbon atoms and 1 atomic vacancy.

^b System B: Supercell with 161 carbon atoms and 1 atomic vacancy.

^c System C: Supercell with 160 carbon atoms and 2 atomic vacancies ca. 11 apart.

^d System D: Supercell with 160 carbon atoms and 2 atomic vacancies ca. 4.5 apart.

^e System E: Supercell with 96 carbon atoms with zigzag edges partially passivated by 16 oxygen atoms.

There were some variations in the average B_{hf} values as well as in the total magnetic moments of each system due to the possible interactions between neighbor atomic magnetic moments. As an example, the comparison between systems containing a single atomic vacancy (systems A and B, as described in Table I) showed a slightly reduced B_{hf} value for the larger supercell, corresponding to the larger separation between each defect and its image produced by the use of periodic boundary conditions in the DFT calculations. Similarly, in the case of two interacting single vacancies (systems C and D), the B_{hf} and the total magnetic moment were found to increase with the reduction in the separation between the two ferromagnetically-coupled vacancies. The largest total magnetic moments and B_{hf} values among the studied systems were found for the graphite nanoribbon, where the magnetic response is the result of the ferromagnetic coupling between the magnetic moments associated with dangling bonds at edge sites⁵.

Guided by these DFT calculations, zero-field NMR experiments were then carried out in a frequency range encompassing the resonance frequencies corresponding to the predicted B_{hf} values. Using the well-known magnetogyric ratio of ^{13}C (10.569 MHz/T)²³, these frequencies were estimated in the range 200-230MHz. A significant zero-field NMR signal was indeed found at frequencies just above this range at 1.5K (Fig.2a); by sweeping the frequency, the maximum signal was detected at a frequency of ca. 260MHz, as shown in the NMR spectrum exhibited in Fig.2b. The B_{hf} value corresponding to this peak is around 24T; the deviation from the calculated

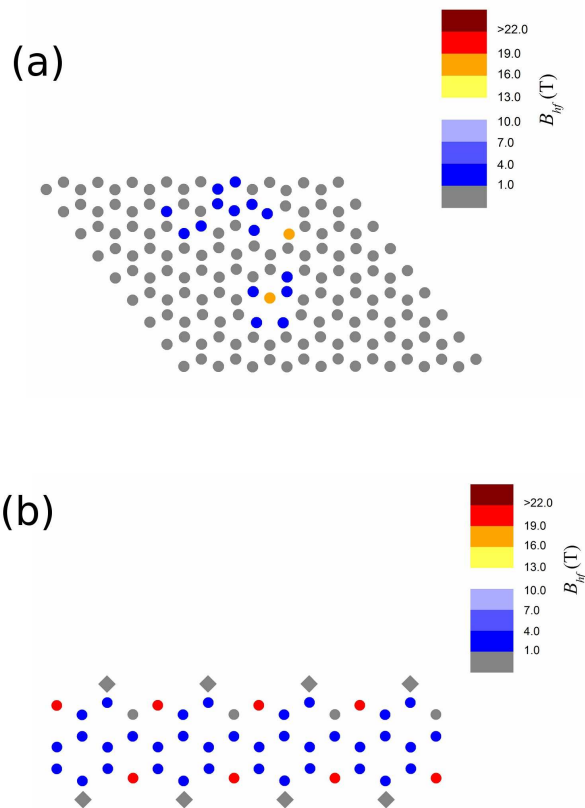


FIG. 1. Colormaps showing the distribution of calculated B_{hf} values for system C (graphene sheet with two atomic vacancies ca. 11 Å) (a) and along a single graphene layer in system E (graphite nanoribbon) (b). The circles represent carbon atoms and the diamonds in (b) represent oxygen atoms.

values given in Table 1 is not surprising, considering the complexity of the real material (from the chemical, structural and magnetic points of view) in comparison to the idealized model systems used in the DFT calculations. The NMR spectrum shown in Fig. 2 was fitted by using two Gaussian lines, named lower (L) and upper (U) lines, with different intensities (L being thus the dominant contribution in zero-field NMR spectra). The dependence of L peak intensity on RF pulse field amplitude B_1 (Fig. 2b, inset) clearly did not follow the usual sinusoidal curve observed in diamagnetic materials: this is characteristic of NMR in ferromagnets and is caused by B_1 and signal enhancement due to the oscillation of large electronic magnetic moments specially in domain walls²¹. A $\pi/2$ pulse in the regular sense is thus not well defined, making absolute intensity comparison between different lines somewhat ambiguous; this problem was exacerbated in NMR experiments performed under external magnetic fields, as discussed below. However, the shape of the echo intensity versus B_1 curve is strong evidence that the observed spectrum was indeed asso-

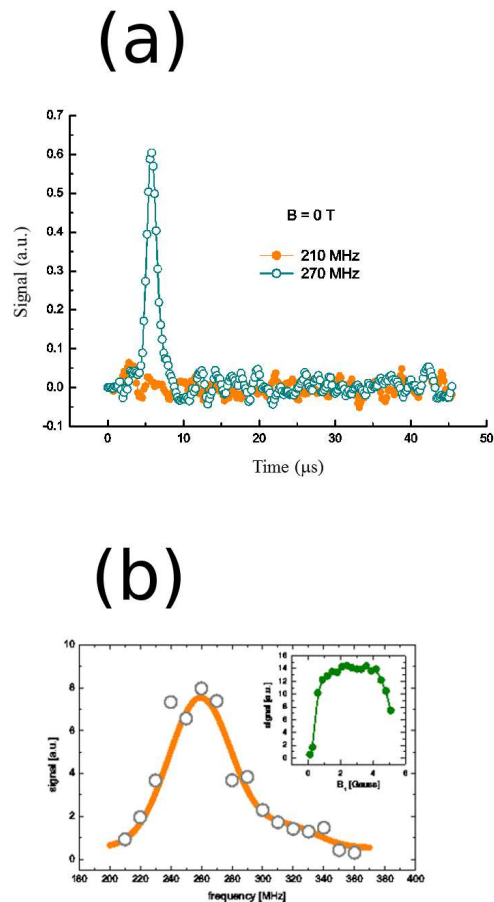


FIG. 2. (a) Raw time-domain zero-field NMR signal due to ^{13}C nuclei in ferromagnetic graphite at two frequencies (full symbols 210 MHz, empty symbols 270 MHz). The spin echo is clearly visible at 270 MHz, whereas the 'blank' measurement at 210 MHz demonstrates the absence of any spurious baseline signals. This zero-field NMR signal is strong evidence of a large and intrinsic hyperfine magnetic field at the carbon sites. b) ^{13}C zero-field NMR spectrum, obtained by integrating spin echoes at different frequencies. The measurement was performed at 1.5 K. Two distinct NMR lines are resolved, the faint upper (U) and much stronger lower (L) line (the solid line is a double gaussian fit). Inset shows the dependence of signal intensity on the excitation pulse strength, with a shape characteristic of ferromagnetic materials.

ciated with the ferromagnetic-enhanced response due to ^{13}C nuclei in ferromagnetic graphite. It is worth noting that the features of the NMR spectrum shown in Fig. 2 were well reproduced in an independent experiment performed with a second ferromagnetic graphite sample from another batch, confirming the robustness of the method of sample preparation and the intrinsic character of the zero-field NMR signal detected in this material.

The relative intensities of the U and L lines were found

to change dramatically with the application of small external magnetic fields (Fig. 3), suggesting a different origin for the L and U signals. The monotonous drop of the L signal intensity suggests that the L line originates from nuclei in Bloch walls, since the number of domains is expected to decrease with increasing external field. Following this simple reasoning, the U line would be due to ^{13}C nuclei inside ferromagnetic domains. Accordingly, the peak position of this line was found to shift by ca. 10MHz in an external field of 1T, following the shift expected based on the magnetogyric ratio of ^{13}C nuclei for the case where the external magnetic field is collinear with the hyperfine magnetic field.

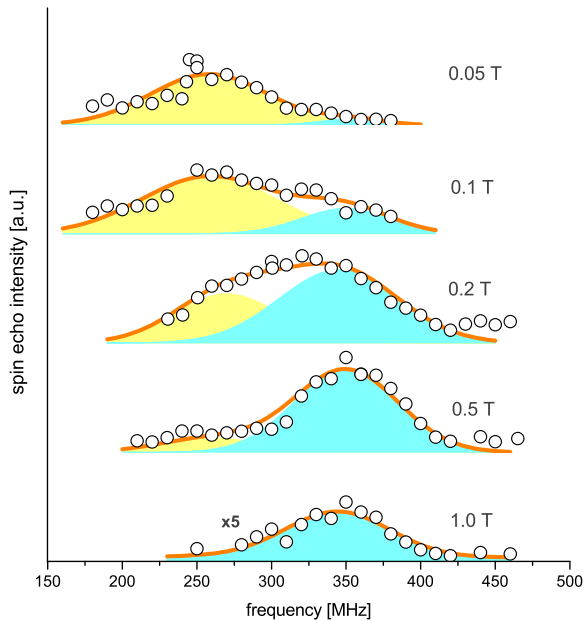


FIG. 3. ^{13}C NMR spectra recorded under several external magnetic fields for ferromagnetic graphite, at 1.5 K. The spectrum at 1 T is magnified five times for clarity. Solid lines are double Gaussian fits. The two NMR lines observed in zero field show rather different behavior in applied fields, indicating a difference in their origin.

In summary, ^{13}C NMR experiments performed under zero or small applied magnetic fields in conjunction with DFT calculations carried out in model systems allowed the direct evaluation of the hyperfine magnetic field in a ferromagnetic carbon-based material, opening the possibility of more in-depth studies of the hyperfine interaction in carbon materials presenting magnetic properties.

ACKNOWLEDGMENTS

The authors thank Damir Paji (from the Laboratory for magnetic measurements at the University of Zagreb) for the SQUID magnetization measurements. JCCF and

WLS are grateful to Prof. Tito Bonagamba (from the Physics Institute of So Carlos, University of So Paulo, Brazil) for his help with the development of the computational infrastructure used in this work. The financial support from the agencies FAPES, FAPESP, FINEP, CAPES and CNPq (Brazil) and HRZZ (Croatia) is also gratefully acknowledged.

REFERENCES

- ¹O. V. Yazyev, Emergence of magnetism in graphene materials and nanostructures. *Rep. Prog. Phys.* 73, 056501 (2010).
- ²P. Recher, B. Trauzettel, Quantum dots and spin qubits in graphene. *Nanotechnology* 21, 302001 (2010).
- ³T. L. Makarova, Magnetic properties of carbon structures. *Semiconductors* 38, 615-638 (2004).
- ⁴R. R. Nair, M. Sepioni, I.-L. Tsai, O. Lehtinen, J. Keinonen, A. V. Krasheninnikov, T. Thomson, A. K. Geim, I. V. Grigorieva, Spin-half paramagnetism in graphene induced by point defects. *Nature Phys.* 8, 199-202 (2012).
- ⁵D. W. Boukhvalov, S. Moehlecke, R. R. da Silva, Y. Kopelevich, Effect of oxygen adsorption on magnetic properties of graphite. *Phys. Rev. B* 83, 233406 (2011).
- ⁶M. M. Ugeda, I. Brihuega, F. Guinea, J. M. Gomez-Rodriguez, Missing atom as a source of carbon magnetism. *Phys. Rev. Lett.* 104, 096804 (2010).
- ⁷A. W. Momb, H. Pardo, R. Faccio, O. F. de Lima, E. R. Leite, G. Zanelatto, A. J. C. Lanfredi, C. A. Cardoso, F. M. Arajo-Moreira, Multilevel ferromagnetic behavior of room-temperature bulk magnetic graphite. *Phys. Rev. B* 71, 100404(R) (2005).
- ⁸W. S. Paz, W. L. Scopel, J. C. C. Freitas, On the connection between structural distortion and magnetism in graphene with a single vacancy. *Solid State Commun.* 175-176, 71-75 (2013).
- ⁹O. A. Yazyev, Hyperfine interactions in graphene and related carbon nanostructures. *Nano Lett.* 8, 1011-1015 (2008).
- ¹⁰B. E. Kane, A silicon-based nuclear spin quantum computer. *Nature* 393, 133-137 (1998).
- ¹¹P. C. Maurer, G. Kucsko, C. Latta, L. Jiang, N. Y. Yao, S. D. Bennett, F. Pastawski, D. Hunger, N. Chisholm, M. Markham, D. J. Twitchen, J. I. Cirac, M. D. Lukin, Room-temperature quantum bit memory exceeding one second. *Science* 336, 1283-1286 (2012).
- ¹²B. Dra, F. Simon, Unusual hyperfine interaction of Dirac electrons and NMR spectroscopy in graphene. *Phys. Rev. Lett.* 102, 197602 (2009).
- ¹³M. Ricc, D. Pontiroli, M. Mazzani, M. Choucair, J. A. Stride, O. V. Yazyev, Muons probe strong hydrogen interactions with defective graphene. *Nano Lett.* 11, 4919-4922 (2011).
- ¹⁴S. N. Mishra, S. K. Mohanta, S. M. Davane, S. K. Srisvastava, Defect induced magnetic interactions in highly oriented pyrolytic graphite (HOPG): a local investigation using TDPAD method. *Hyperfine Interact.* 197, 71-75 (2010).
- ¹⁵A. C. Gossard, A. M. Portis, Observation of nuclear resonance in a ferromagnet. *Phys. Rev. Lett.* 3, 164-166 (1959).
- ¹⁶L. J. Bruner, J. I. Budnick, R. J. Blume, Nuclear magnetic resonance of Ni61 in metallic nickel. *Phys. Rev.* 121, 83 (1961).
- ¹⁷J. I. Budnick, L. J. Bruner, R. J. Blume, E. L. Boyd, Nuclear magnetic resonance of Fe57 in unenriched Fe, *J. Appl. Phys.* 32 120S-121S (1961).
- ¹⁸Information on materials and methods are available upon request.
- ¹⁹H. Pardo, R. Faccio, F. M. Arajo-Moreira, O. F. de Lima, A. W. Momb, Synthesis and characterization of stable room temperature bulk ferromagnetic graphite. *Carbon* 44, 565-569 (2006).
- ²⁰F. M. Arajo-Moreira, H. Pardo and A. W. Momb, Process of

- preparing magnetic graphite materials, and material thereof. US Patent 8,303,836 B2 (granted on November, 2012).
- ²¹E. A. Turov, M. P. Petrov, Nuclear magnetic resonance in ferro- and antiferromagnets (Halsted Press, London, 1972).
- ²²Y. Zhang, S. Talapatra, S. Kar, R. Vajtai, S. K. Nayak, P. M. Ajayan, First-principles study of defect-induced magnetism in carbon. *Phys. Rev. Lett.* 99, 107201 (2007).
- ²³R. K. Harris, E. D. Becker, S. M. C. de Menezes, R. Goodfellow, P. Granger, NMR nomenclature. Nuclear spin properties and conventions for chemical shifts (IUPAC recommendations 2001). *Pure Appl. Chem.* 73, 1795-1818 (2001).